

## Geometrically nonlinear thermoelastic analysis of shells: modelling, incremental-iterative solution and reduction technique

LIGUORI F. S.<sup>1, a\*</sup>, MAGISANO D.<sup>1, b</sup>, LEONETTI L.<sup>1, c</sup>, MADEO A.<sup>1, d</sup> and GARCEA G.<sup>1, e</sup>

<sup>1</sup>University of Calabria, DIMES, Ponte P. Bucci, cubo 39 C, 87030, Rende (CS), Italy

<sup>a</sup>francesco.liguori@unical.it, <sup>b</sup>domenico.magisano@unical.it, <sup>c</sup>leonardo.leonetti@unical.it, <sup>d</sup>antonio.madeo81@unical.it, <sup>e</sup>giovanni.garcea@unical.it

**Keywords:** Shell Structures, Thermoelastic Analysis, Geometric Nonlinearity, Buckling, Newton Method, Isogeometric Analysis

**Abstract.** This work presents an accurate and efficient numerical tool for geometrically nonlinear thermoelastic analyses of thin-walled structures. The structure is discretized by an isogeometric solid-shell model avoiding the parameterization of finite rotations. An efficient modeling of thermal strains, temperature-dependent materials and general temperature profiles is proposed. Then, a generalized path-following method is developed for solving the discrete equations with the temperature amplifier as additional unknown. Finally, a reduction technique based on Koiter theory is derived for a quick estimate of the nonlinear thermal buckling.

### Introduction

Civil, aeronautical and mechanical structures can be affected by high temperature rise [1]. The consequent high thermally-induced stresses and degradation of the thermoelastic properties can lead to buckling. Both aspects can significantly influence the buckling point and the postbuckling response. The nonlinear systems of equations defining the structural response can be solved step-by-step by using arc-length continuation method. In geometrically nonlinear analysis for mechanical loads, it has been shown that the use of a mixed formulation with independent stress variables makes the solution method able to withstand much larger step sizes with fewer iterations compared to purely displacement-based formulations [2]. It is also worth mentioning reduced order models based on the FEM implementation of Koiter's theory of elastic stability [3]. This work presents an accurate and efficient numerical tool for geometrically nonlinear thermoelastic analyses of thin-walled structures. The starting point is an accurate isogeometric solid-shell discretization without rotational DOFs. Focus is given to an efficient modelling of thermal strains, temperature-dependent materials and general temperature profiles based on a numerical pre-integration through the shell thickness in a pre-processing stage. Then, a generalized path-following method is developed for solving the discrete equations with the temperature amplifier as additional unknown, in order to trace the temperature-displacement nonlinear curve of the structure also in case of limit points and unstable paths. A consistent definition of the tangent operators and a mixed integration point strategy give a robust analysis with a reduced iterative burden, even in case of complex nonlinear behaviors where well-known simulation codes are outperformed or even fail. Finally, a reduction technique is derived for a quick estimate of the nonlinear thermal buckling point of structures with a high number of discrete degrees of freedom. It is a generalization of the so-called Koiter method to thermoelasticity. Numerical application are given to validate the proposal.



### Solid-shell model with thermal strains and temperature-dependent material properties

This section introduces the main equations of the solid-shell model [4,5] extended to thermoelastic nonlinear analyses. Assuming a linear through-the-thickness interpolation, the position vector  $\mathbf{X}$  and the displacement field  $\mathbf{d}$  are expressed as

$$\mathbf{X} = \mathbf{X}_0 [\xi, \eta] + \frac{2h}{\zeta} \mathbf{X}_n [\xi, \eta], \quad \mathbf{d} = \mathbf{d}_0 [\xi, \eta] + \frac{2h}{\zeta} \mathbf{d}_n [\xi, \eta], \quad (1)$$

with  $h$  the shell thickness. The Green-Lagrange strain components are collected in vector  $\mathbf{E} = [E_{11}, E_{22}, 2E_{12}, E_{33}, 2E_{23}, 2E_{13}]^T$  and linearized with respect to  $\zeta$  as

$$\mathbf{E} \approx \begin{bmatrix} \mathbf{e}[\xi, \eta] + \zeta \boldsymbol{\chi} [\xi, \eta] \\ \mathbf{E}_{33}[\xi, \eta, 0] \\ \boldsymbol{\gamma} [\xi, \eta] \end{bmatrix} \quad (2)$$

Generalised strains (3) presents the same format than in the Mindlin-Reissner model plus the thickness strain  $E_{33}$  but does not requires a direct parameterisation of 3D finite rotations.

Constitutive law, thermal strains and strain energy. We assume only in-plane thermal strains:

$$\mathbf{E}_T = \begin{bmatrix} \boldsymbol{\alpha}_p \\ 0 \\ 0 \end{bmatrix} \mathbf{T} \quad \text{with} \quad \boldsymbol{\alpha}_p = \begin{bmatrix} \alpha_1 \\ \alpha_2 \\ 0 \end{bmatrix} \quad (3)$$

where  $\alpha_1$  and  $\alpha_2$  are the thermal expansion coefficients. The strain energy of the solid-shell model can be written in compact notation as

$$\Phi[\mathbf{d}] \equiv \frac{1}{2} \int_{\Omega} \int_{-\frac{h}{2}}^{\frac{h}{2}} (\mathbf{E} - \mathbf{E}_T[\mathbf{T}])^T \mathbf{C}[\xi, \mathbf{T}] (\mathbf{E} - \mathbf{E}_T[\xi, \mathbf{T}]) \, d\zeta \, d\Omega = \int_{\Omega} \left( \frac{1}{2} \boldsymbol{\varepsilon}^T \mathbf{C}[\mathbf{T}] \boldsymbol{\varepsilon} - \boldsymbol{\varepsilon}^T \boldsymbol{\sigma}_T \right) d\Omega + \text{cost} \quad (4)$$

Let us consider a distribution of temperature increment over the structure  $T[\xi, \eta, \zeta]$  with respect to the ambient value. We can assume

$$T[\xi, \eta, \zeta] = \lambda \hat{T} [\xi, \eta, \zeta]$$

where  $\hat{T} [\xi, \eta, \zeta]$  is the given temperature distribution and  $\lambda$  an amplifier factor. In case of temperature-dependent material properties, the elastic moduli and the thermal expansion coefficients depend on  $T$ . Their laws of variability can be assumed on the basis of experimental results or using formulas available in standards.

From a computational point of view, it is more handy to express  $\mathbf{S}_T = \mathbf{C}[\mathbf{T}] \mathbf{E}_T[\mathbf{T}]$  by means of a polynomial interpolation in  $T$  at some temperatures  $T_k$ , which can be rewritten as

$$\mathbf{C}[\lambda] = \sum_{k=0}^n \lambda^k \hat{\mathbf{C}}_k \hat{T}^k, \quad \mathbf{S}_T[\lambda] = \sum_{k=0}^n \lambda^k \hat{\mathbf{S}}_{T_k} \hat{T}^k \quad (5)$$

This choice makes it possible to express the generalised quantities of the solid-shell model  $\mathbf{C}[\mathbf{T}]$  and  $\boldsymbol{\sigma}_T$  as a function of  $\lambda$  by a numerical through-the-thickness integration carried out once and for all in a pre-processing stage, regardless of the complexity of  $\hat{T} [\xi, \eta, \zeta]$ .

### The isogeometric solid-shell discretisation

The continuum solid-shell model is approximated over the shell mid-surface by using NURBS functions, following the approach proposed in [4,5] to which we refer for further details.

Geometry and displacement fields are described as

$$\mathbf{X}[\xi, \eta, \zeta] = \mathbf{N}_d[\xi, \eta, \zeta] \mathbf{X}_e, \quad \mathbf{d}[\xi, \eta, \zeta] = \mathbf{N}_d[\xi, \eta, \zeta] \mathbf{d}_e. \quad (6)$$

where  $\mathbf{X}_e = [\mathbf{X}_{0e}, \mathbf{X}_{ne}]$  and  $\mathbf{d}_e$  collects the control points. The matrix  $\mathbf{N}_d[\xi, \eta, \zeta]$  collects the interpolation functions

$$\mathbf{N}_d[\xi, \eta, \zeta] = \left[ \mathbf{N}[\xi, \eta] \quad 2 \frac{\zeta}{h} \mathbf{N}[\xi, \eta] \right] \quad (7)$$

where  $\mathbf{N}[\xi, \eta]$  are 2D NURBS functions of the middle surface coordinates only. By exploiting Eq.(3) we obtain the generalised strain-displacement relationship. An efficient patch-wise integration schemes [4,5] to avoid membrane and shear locking is adopted for numerical integration. In this work, we adopt cubic  $C^2$  NURBS with the integration scheme named  $S_1^4$ .

### The MIP arc-length continuation method for thermoelastic nonlinear analyses

We consider a slender hyperelastic structure subject to a conservative load  $\mathbf{p}$  and to a temperature rise defined as  $T[\xi, \eta, \zeta] = \lambda \hat{T}[\xi, \eta, \zeta]$ . The equilibrium condition is given by the virtual work equation in discrete form

$$\mathbf{r}[\mathbf{u}, \lambda] \equiv \mathbf{s}[\mathbf{u}, \lambda] - \mathbf{p} = \mathbf{0} \quad (8)$$

where  $\mathbf{r}: \mathbb{R}^{n+1} \rightarrow \mathbb{R}^n$  is a nonlinear vectorial function of the vector  $[\mathbf{u}, \lambda] \in \mathbb{R}^{n+1}$ , collecting the discrete DOFs  $\mathbf{u} \in \mathbb{R}^n$  and the multiplier  $\lambda \in \mathbb{R}$ . Eq.(8) represents a system of n-equations and n+1 unknowns and defines the equilibrium path as a curve in the  $[\mathbf{u}, \lambda]$  space.

Letting  $\mathbf{x} = \{\mathbf{u}, \lambda\}$ , a new equilibrium point  $\mathbf{x}^{k+1}$  is obtained starting from the previous known point  $\mathbf{x}_0 = \mathbf{x}^{(k)}$  by solving iteratively the equilibrium equations plus the arc-length constraint for an assigned value of  $\Delta\xi$

$$\begin{cases} \mathbf{r}[\mathbf{u}, \lambda] \equiv \mathbf{s}[\mathbf{u}, \lambda] - \mathbf{p} = \mathbf{0} \\ \mathbf{r}_\lambda[\mathbf{u}, \lambda] \equiv \mathbf{n}_x^T \mathbf{M}_x (\mathbf{x} - \mathbf{x}_0) - \Delta\xi = \mathbf{0} \end{cases} \quad \Delta\xi = \mathbf{n}_x^T \mathbf{M} (\mathbf{x}_1 - \mathbf{x}_0) \quad (9)$$

with  $\mathbf{x}_1$  the first predictor. The most simple arc-length equation is an adaptive hyperplane with  $\mathbf{M}_x$  a suitable metric matrix and  $\mathbf{n}_x$  its normal vector. Introducing the following tangent operators

$$\mathbf{K} \equiv \frac{\partial \mathbf{s}[\mathbf{u}, \lambda]}{\partial \mathbf{u}} \quad \hat{\mathbf{s}} \equiv \frac{\partial \mathbf{s}[\mathbf{u}, \lambda]}{\partial \lambda} \quad (10)$$

Newton iterations can be then used to solve the extended nonlinear system of equations (9).

As shown in [2], the Newton method convergence depends on how rapidly the iteration matrix changes with respect to the configuration variables  $\mathbf{u}$ . The MIP Newton method using displacements and independent stress DOFs, makes the Newton method able to withstand very large steps with a very small iterative effort.

The strain energy is rewritten in a Hellinger-Reissner mixed format using a MIP strategy. The stress field is not interpolated, but the stresses at each integration point  $\boldsymbol{\sigma}_g$  are taken directly as independent variables. In particular, by relaxing the constitutive law at each integration point one obtains the pseudo Hellinger-Reissner energy

$$\Phi_e[\mathbf{u}_e, \lambda] = \left\{ \sum_g \boldsymbol{\sigma}_g^T (\boldsymbol{\varepsilon}_g - \mathbf{C}_g^{-1}[\lambda] \boldsymbol{\sigma}_{Tg}) - \frac{1}{2} \boldsymbol{\sigma}_g^T \mathbf{C}_g^{-1}[\lambda] \boldsymbol{\sigma}_g \right\} w_g \quad (11)$$

Due to the local nature of the stress variables, decoupled at each IP, they can be condensed out when solving the linear systems and are then not involved in the global operations.

### A Koiter-inspired reduction technique

A reduced order model (ROM) is proposed for an efficient nonlinear thermoelastic analysis of structure prone to buckling using a generalisation of the so-called Koiter method [3,5] to include thermal effects. The difficulty of this extension is due to the nonlinear dependence of the strain energy from the parameter  $\lambda$  that regulates the temperature rise. In particular, an accurate and coherent ROM requires the solution of an accurate 2-point linearized buckling problem in mixed (stress-displacement) form.

The space of admissible configuration, following a Galerkin approach, is limited to the following reduced model

$$\mathbf{u}_d = \mathbf{u}_f[\lambda] + \mathbf{v}[\mathbf{t}] + \frac{1}{2} \mathbf{w}[\lambda, \mathbf{t}] \tag{12}$$

where  $\mathbf{u}_f[\lambda] = \lambda \hat{\mathbf{u}}$  is the solution along the initial path tangent,  $\mathbf{v}[\mathbf{t}] = \sum_i t_i \hat{\mathbf{v}}_i$  is a combination of buckling modes corresponding to the first  $m$  linearized critical temperatures and  $\mathbf{w} = \sum_i \sum_j t_i t_j \mathbf{w}_{ij} + \lambda^2 \hat{\mathbf{w}}$  is the corresponding orthogonal second order correction.

Introducing the approximation of  $\mathbf{u}_d$  in the discrete equilibrium equation using  $\hat{\mathbf{v}}_i$  as test functions according to a Ritz-Galerkin approach and expanding in Taylor series up to the 3rd order in  $\lambda$  and  $t_i$ , we obtain the nonlinear reduced equations

$$r_i[\mathbf{t}, \lambda] = 0 \quad i = 1 \dots n \tag{13}$$

Equations (13) are an algebraic nonlinear system of  $m$  equations in the  $m+1$  variables  $\lambda, t_1 \dots t_m$  with known coefficients and can be solved using a path-following algorithm. Because of the small size of the system, the solution is very fast.

### Numerical results

The performance of the proposed formulation is herein tested. The efficiency of the MIP strategy is compared with a displacement-based Newton method. Additionally, comparison is made with the nonlinear analysis implemented in the commercial code Abaqus and shell finite element S8R. A linear temperature distribution  $\hat{T}(\zeta) = T_M + \frac{2\zeta}{h} T_L$  is assumed through the shell thickness. Additional tests are reported in [6,7].

A simply-supported Euler beam-like structure, reported in Fig.1, is considered. The length is  $L = 10^3 \text{ mm}$  and different values of  $L/h$  are analysed. Temperature-dependent material properties are considered and reported in details in [6,7,8]. The structure is subject to an initial compression load  $q = 0.95 k_c$ , with  $k_c = \pi^2 h^3 E_0 / (12 L^2)$ . Subsequently, a temperature change is applied, with  $T_M = 1$  and different values of the through-the-thickness gradient  $T_L$ .

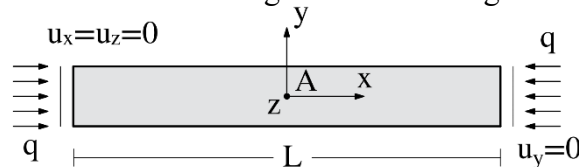


Figure 1 Euler beam: geometry, loads and boundary conditions.

It is worth noting that the structure does not exhibit any additional stress due to the temperature rise. Conversely, since the material properties are temperature-dependent, the temperature rise reduces the beam stiffness leading to buckling. Figure 2 depicts the equilibrium paths for three different values of  $T_L$  obtained through the proposed model and Abaqus which fails to reach convergence beyond the bifurcation load. Interestingly, its last converged point is characterized by a decreasing temperature for increasing values of  $T_L$ . This is likely due to an approximated evaluation of the tangent operators for TD material properties.

Table 1 compares the number of iterations required by Newton and MIP Newton for different values of  $L/h$ . The Newton method performances drastically deteriorate for increasing values of  $L/h$  and convergence is no longer possible starting from  $L/h=10^3$ . Conversely, MIP Newton is not influenced by the slenderness ratio.

Table 1. Euler beam: steps and iterations for Newton and MIP Newton with  $T_L = 10^{-4}$ .

$L/h$	Newton		MIP Newton		
	steps	iterations	steps	iterations	elapsed time*
30	110	368	52	131	0.33
100	158	577	48	121	0.21
1000		fails	36	95	-

\* normalised with respect to Newton's elapsed time

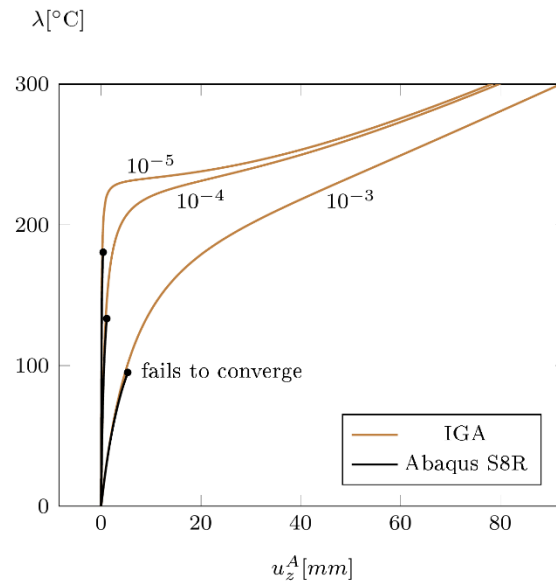


Figure 2. Euler beam: equilibrium paths for different values of the through-the-thickness temperature gradient and  $L/h=100$ .

Furthermore, it is possible to observe that the proposed Koiter reduced formulation with just one mode (and relative corrective) is pretty accurate in all cases up to significant post-buckling deformations.

### Conclusions

The paper presented a robust and efficient simulation tool for the nonlinear thermoelastic analysis of thin-walled structures. The first part of the work consisted in developing a solid-shell isogeometric discretisation which requires a low number of displacement DOFs for accurately describing the shell kinematics. Focus was given to the modelling of thermal strains and temperature-dependent materials within the solid-shell concept. A reduction technique based on the Koiter method was also proposed and applied to buckling problems. Tests on composite shells and thin-walled structures are available in [6,7].

### References

- [1] M. Bhatia, E. Livne (2008), Design-oriented thermostructural analysis with internal and external radiation, part 1: Steady state, AIAA Journal 46 (3), 578–590. <https://doi.org/10.2514/1.26236>
- [2] D. Magisano, L. Leonetti, G. Garcea (2017), How to improve efficiency and robustness of the Newton method in geometrically non-linear structural problem discretized via displacement-based finite elements, Computer Methods in Applied Mechanics and Engineering 313, 986-1005. <https://doi.org/10.1016/j.cma.2016.10.023>

- [3] G. Garcea, F. S. Liguori, L. Leonetti, D. Magisano, A. Madeo, (2017), Accurate and efficient a posteriori account of geometrical imperfections in Koiter finite element analysis, *International Journal for Numerical Methods in Engineering* 112, 1154–1174. <https://doi.org/10.1002/nme.5550>
- [4] L. Leonetti, F. Liguori, D. Magisano, G. Garcea (2018), An efficient isogeometric solid-shell formulation for geometrically nonlinear analysis of elastic shells, *Computer Methods in Applied Mechanics and Engineering* 331, 159-183. <https://doi.org/10.1016/j.cma.2017.11.025>
- [5] L. Leonetti, D. Magisano, F. Liguori, G. Garcea (2018), An isogeometric formulation of the Koiter's theory for buckling and initial post-buckling analysis of composite shells, *Computer Methods in Applied Mechanics and Engineering* 337, 387-410. <https://doi.org/10.1016/j.cma.2018.03.037>
- [6] F. S. Liguori, D. Magisano, L. Leonetti, G. Garcea (2021), Nonlinear thermoelastic analysis of shell structures: solid-shell modelling and high-performing continuation method, *Composite Structures* 266, 113734. <https://doi.org/10.1016/j.compstruct.2021.113734>
- [7] F. S. Liguori, D. Magisano, A. Madeo, L. Leonetti, G. Garcea (2022), A Koiter reduction technique for the nonlinear thermoelastic analysis of shell structures prone to buckling, *International Journal for Numerical Methods in Engineering* 123 (2), 547-576. <https://doi.org/10.1002/nme.6868>
- [8] J. Lee, M. Bhatia (2019), Impact of corrugations on bifurcation and thermoelastic responses of hat-stiffened panels, *Thin-Walled Structures* 140, 209-221. <https://doi.org/10.1016/j.tws.2019.03.027>